JOURNAL OF GEOPHYSICAL RESEARCH, VOL. 94, NO. D15, PAGES 18,305-18,326, DECEMBER 20, 1989

THE GLOBAL GEOCHEMISTRY OF BOMB-PRODUCED TRITIUM: GENERAL CIRCULATION MODEL COMPARED TO AVAILABLE OBSERVATIONS AND TRADITIONAL INTERPRETATIONS

Randal D. Koster, Wallace S. Broecker,[2] Jean Jouzel,[3,4] Robert J. Suozzo,[5]
Gary L. Russell,[6] David Rind,[6] and James W. C. White[7]

Abstract. Observational evidence suggests that of the tritium produced during nuclear bomb tests that has already reached the ocean, more than twice as much arrived through vapor impact as through precipitation. In the present study, the Goddard Institute for Space Studies 8°x10° atmospheric general circulation model is used to simulate tritium transport from the upper atmosphere to the ocean. The simulation indicates that tritium delivery to the ocean via vapor impact is about equal to that via precipitation. The model result is relatively insensitive to several imposed changes in tritium source location, in model parameterizations, and in model resolution. Possible reasons for the discrepancy are explored.

1. Introduction

One of the major challenges in creating a valid general circulation model (GCM) of the atmosphere is obtaining a correct simulation of the Earth's hydrologic cycle. Unfortunately, a paucity of real world water flux measurements prevents an adequate, complete evaluation of any GCM's inherent hydrologic cycle. Modelers can only say that their simulations produce certain specific hydrologic quantities (such as surface precipitation fields) that match reasonably well those observed in nature. While it is tempting to conclude from such a match that all important aspects of the water cycle are therefore properly modeled, the modelers cannot ascertain the extent to which the match results from the tuning of inadequate model parameterizations.

One method of testing the hydrologic cycles of GCMs is to simulate the transport of the tritiated (HTO) water produced by bomb tests from the stratosphere to the ocean. This transport involves virtually all the elements of the hydrologic cycle (e.g., vapor transport, cloud formation, precipitation, soil water, and runoff). By comparing the pathways followed by tritium through the model with those followed in the real world, the reliability of at least certain aspects of the model water cycle can be checked.

The work presented in this initial paper focuses on one particular aspect of tritium transport, namely the role of vapor impact in the delivery of tritium from the atmosphere to the ocean surface. Craig and Gordon [1965] first pointed out the importance of this mode of delivery and provided a method for quantifying it. The flux compilations of Weiss and Roether [1980] constructed with Craig's method suggest that for the northern hemisphere Atlantic and Pacific oceans, 2.4 times as much tritium has reached the ocean surface through surface vapor exchange as through precipitation. Because precipitation and river runoff appear to account for only about 30% of the tritium found in the sea [Weiss and Roether, 1980; Broecker et al., 1986], delivery by vapor impact is the logical candidate to supply the other 70% of the ocean tritium inventory.

The tritium input flux ratio of 2.4 is precisely the quantity that the Goddard Institute for Space Studies (GISS) GCM attempted to reproduce. As will be seen, the GCM produces a ratio no more than half this great. It will also be shown, however, that the discrepancy does not necessarily prove that the GCM behaves incorrectly. In light of the uncertainties inherent in the observational analysis, the GCM analysis can perhaps be viewed not as a test of the GCM's hydrological cycle but as an alternative method for estimating the tritium fluxes.

2. The Weiss and Roether Tritium Input Scenario

In their calculation of the amount of bomb-produced tritium added to the sea, Weiss and Roether [1980] utilize annual oceanic evaporation and precipitation averaged over 5° latitudinal bands, as provided by Baumgartner and Reichel [1975]. Values for the northern hemisphere Atlantic and Pacific oceans are reproduced in Table 1. Weiss and Roether also list as a function of latitude their estimates of total tritium deposition I_{EP} into these oceans.

Weiss and Roether compute tritium deposition through the equation

$$I_{EP} = (PC_p + E\frac{h}{1-h}C_V - E\frac{1}{\alpha(1-h)}C_s)A \qquad (1)$$

The first term is the precipitation input; P and C_p are observed latitude-dependent precipitations and tritium concentrations in precipitation, respectively. The second term is the Craig and

[1]Hydrological Sciences Branch, NASA Goddard Space Flight Center, Greenbelt, Maryland.
[2]Lamont-Doherty Geological Observatory of Columbia University, Palisades, New York.
[3]Laboratoire de Geochimie Isotopique, Centre National de la Recherche Scientifique, Departement de Physico-Chimie, Commissariat a l'Energie Atomique, Gif sur Yvette, France.
[4]Also at Laboratoire de Glaciologie et de Geophysique de l'Environnement, Centre National de la Recherche Scientifique, France.
[5]S T Systems Corp., New York
[6]NASA Goddard Institute for Space Studies, New York
[7]University of Colorado, Boulder.

Paper number 89JD00813.
0148-0227/89/89JD-00813$05.00

TABLE 1. Summary of Flux Compilations of Weiss and Roether [1980]

Latitude Band, deg	E, m/yr	P, m/yr	Total Input of Tritium, MCi	Precipitation Input, MCi	Vapor Input, MCi	Ratio	Percent of Total
			Tritium in North Atlantic				
75-80	0.18	0.26	9.5	3.7	6.5	1.8	1.71
70-75	0.34	0.34	24.9	7.6	19.4	2.6	4.52
65-70	0.44	0.53	32.0	10.7	22.6	2.1	5.59
60-65	0.59	0.97	44.4	18.8	29.1	1.5	8.03
55-60	0.77	1.02	53.3	19.9	38.2	1.9	9.74
50-55	0.93	1.18	47.9	17.6	35.2	2.0	8.84
45-50	0.98	1.14	46.3	15.9	34.8	2.2	8.50
40-45	1.19	1.00	55.2	15.4	46.5	3.0	10.36
35-40	1.53	0.82	46.4	9.3	43.9	4.7	8.89
30-35	1.62	0.63	42.2	6.7	43.6	6.5	8.42
25-30	1.53	0.64	37.8	6.6	40.2	6.1	7.83
20-25	1.53	0.52	28.0	4.4	32.5	7.4	6.17
15-20	1.53	0.68	20.5	4.0	22.7	5.7	4.46
10-15	1.46	1.01	14.3	4.2	15.4	3.7	3.29
5-10	1.33	1.69	9.3	3.9	7.8	2.0	1.96
0-5	1.20	1.45	7.5	3.3	7.0	2.1	1.72
Totals				152.0	445.5		
Tritium input ratio for North Atlantic						2.93	
			Tritium in North Pacific				
75-80	0.00	0.00	0.00	0.0	0.0	0.0	0.00
70-75	0.00	0.00	0.00	0.0	0.0	0.0	0.00
65-70	0.00	0.00	0.00	0.0	0.0	0.0	0.00
60-65	0.24	0.61	7.69	3.9	3.9	1.0	1.04
55-60	0.34	1.15	37.49	22.0	16.5	0.8	5.08
50-55	0.48	1.41	53.52	29.6	25.6	0.9	7.30
45-50	0.67	1.46	67.03	32.3	37.7	1.2	9.25
40-45	0.93	1.34	70.58	27.2	48.0	1.8	9.94
35-40	1.13	1.17	72.45	22.9	56.3	2.5	10.47
30-35	1.34	1.01	70.92	18.3	61.8	3.4	10.59
25-30	1.51	0.82	61.55	12.9	60.1	4.7	9.64
20-25	1.62	0.83	57.49	12.0	59.5	5.0	9.45
15-20	1.60	1.13	55.21	13.7	49.2	3.6	8.31
10-15	1.46	1.75	49.92	18.5	39.3	2.1	7.64
5-10	1.30	2.57	45.25	23.2	29.9	1.3	7.02
0-5	1.20	1.81	25.42	12.1	20.3	1.7	4.28
Totals				248.7	508.2		
Tritium input ratio for North Pacific						2.04	
Total precipitation input of tritium for North Atlantic+Pacific				401			
Total vapor input of tritium for North Atlantic+Pacific					954		
Resulting tritium input ratio for North Atlantic+Pacific						2.4	

For each 5°latitudinal band in each ocean, the first three data columns show the average evaporation and precipitation rates used and Weiss and Roether's estimates of the tritium input I_{EP} (equation (1)). The fourth and fifth data columns show the precipitation and downward vapor exchange tritium inputs computed with the first two terms of (1). (These were not tabulated by Weiss and Roether.) The sixth data column provides the ratio of the vapor exchange input to the precipitation input. The final column indicates the percent of total tritium deposited into each band.

Gordon [1965] relationship for downward isotope vapor flux, with E being the net evaporation rate, h the specific humidity of the air 10 m above the ocean divided by the saturated specific humidity at the ocean-air interface, and C_V the concentration of tritium in ocean vapor. Weiss and Roether assumed h to be uniform over the ocean surface with a value of 0.74. Since very few ocean vapor tritium measurements were available to produce average values of C_V versus latitude during the period of peak bomb tritium delivery to the ocean (1963 to 1967), Weiss and Roether assumed that the concentrations of tritium in ocean precipitation and ocean vapor were roughly in isotopic equilibrium, i.e., that $C_V \approx C_P/\alpha$, where α is tritium's liquid/vapor fractionation factor.

They justified this assumption through measurements on vapor/rain pairs collected in the North Atlantic. The value of α was taken to be 1.12 everywhere. The final term in equation (1) is the upward tritium flux, which is proportional to C_S, the tritium concentration in the ocean. A is the area of the latitudinal band.

Table 1 lists by latitude the time-integrated values of I_{EP} computed by Weiss and Roether and also lists the values of the time-integrated precipitation and downward vapor exchange tritium fluxes. (The separate fluxes were not provided in Weiss and Roether's tables.) The precipitation and vapor exchange contributions are summed over the latitudes, and the totals for each ocean are provided at the bottom of Table 1. In the northern hemisphere Atlantic Ocean, 2.9 times as much tritium entered the ocean via vapor exchange than via precipitation. In the northern hemisphere Pacific Ocean, 2.0 times as much entered via vapor exchange than via precipitation. When the two oceans are considered together, the vapor exchange input of tritium is seen to be 2.4 times the precipitation input.

The assumptions leading to the ratio of 2.4, in particular the assumption of isotopic equilibrium between ocean vapor and rain and the neglecting of seasonal correlations, bear further scrutiny and will be discussed again in section 4 of this paper.

3. General Circulation Model Simulation of Tritium Delivery

A set of tritium simulations was run with a version of model II of the GISS GCM to compare the relative importance of the model's precipitation and vapor exchange removal mechanisms with the Weiss and Roether result. The structure and resulting climate patterns of model II are described in detail by Hansen et al. [1983]. The GCM features grid squares with realistic topography, each divided into appropriate fractions of open ocean, sea ice, permanent land ice, and earth. Model II has annual and diurnal cycles driven by solar radiation at the top of the atmosphere. Arakawa's [1972] second-order B grid scheme is used for the dynamics. The radiation parameterization uses the cloud cover and vertical distribution computed by the model.

The particular version of the model used in this study can follow tracers in their travels around the globe. The model atmosphere is initialized with a specific three-dimensional tracer distribution. At every time step in the simulation, the model determines how much tracer enters or leaves a given grid box via advection by the model winds, how much leaves the grid box with precipitating grid box water or enters with reevaporated precipitation, and so forth. Effectively, every model process that can transport model water from one grid box to the next can also transport tracer. A tracer can leave the atmosphere by precipitating to the surface, by condensing onto ocean ice or land, or by undergoing vapor impact at the ocean surface. Diffusion of water or tracer is not modeled explicitly. The presence of tracer does not affect the thermodynamics, the water motion, or any other aspect of the model's general circulation.

The formulations of the various tracer transport processes were thoroughly discussed by Jouzel et al. [1987], who tested the model's ability to reproduce the global distributions of stable water isotopes (HDO, $H_2{}^{18}O$), and by Koster et al. [1988], who used the model to study tracer water transport. Koster et al. [1986] used the model to determine the regional evaporative sources of model precipitation water for selected grid squares. Since the simulation experiments discussed below focus on the relative input of a tracer (HTO) into the ocean through vapor exchange with that through precipitation, the parameterizations of these particular processes bear further discussion.

During large-scale condensation events, some of the tracer vapor in a grid box condenses and falls into the next lower grid box, where it might partially reevaporate. The remaining tracer liquid can partially equilibrate with the surrounding vapor before falling further. Physically, equilibration corresponds to tracer vapor exchange at the surface of the precipitation droplets. If, for example, the tracer/water ratio in the droplet is too large compared to that in the surrounding vapor, net tracer will move from the droplet to the vapor until the ratios are at equilibrium. The fraction of liquid equilibrating, which physically is a function of the droplet size spectrum, can be assigned any value in the model; for large-scale condensation events, the standard model allows all of the liquid to equilibrate. No equilibration is allowed for solid condensate.

Tracer behavior during moist convective events parallels that during large-scale condensation in terms of the equilibration and reevaporation of falling tracer condensate. In moist convective events, however, a plume forms from a portion (normally one-half) of a grid box and carries water vapor and tracer vapor to higher levels before some of it condenses, allowing for a more complete vertical redistribution of tracer. Also, equilibration and reevaporation occur in only a fraction of each lower grid box. Normally, this fraction is one-fourth for boxes above the cloud base and one-half for boxes below. In the standard model, only half of the falling liquid tracer condensate can equilibrate with tracer in surrounding vapor.

Vapor exchange of tracer over an ocean surface proceeds in a direction independent of net water vapor flux. That is, tracer vapor can move downward into the ocean in the presence of a net upward flux of evaporating water. Evaporation of water from an ocean surface in the GCM is calculated as

$$E = \rho\, C_q\, V_s\, (q_g - q_s) \qquad (2)$$

where ρ is the air density, C_q is a drag coefficient, V_s is the surface wind velocity, q_g is the surface specific humidity, and q_s is the specific humidity at the top of the ocean's surface boundary layer. Interpreting this as the sum of upward and downward dynamical fluxes, the downward flux of tracer into the ocean follows naturally as

$$E_{T,\,down} = -\rho\, C_q\, V_s\, q_{st} \qquad (3)$$

where q_{st} is the specific humidity of tracer at the top of the ocean's surface boundary layer.

The surface boundary layer is a parameterized portion of the first GCM model layer lying just above the ocean surface. The specific humidity at the top of the boundary layer for either water or tracer is effectively calculated as a weighted average of the corresponding first model layer and surface specific humidities, the weighting depending in part on the wind speed and the surface roughness. For the tracer studies discussed in this paper, the concentration of tracer in ocean water (and thus the upward dynamical tracer flux) is neglected; as suggested by Table 1 the upward tritium flux would contribute only small amounts to the precipitation and downward vapor exchange fluxes, thereby having only a slight effect on their relative magnitudes. To ensure that the model results are not based on a faulty parameterization of precipitation formation or surface vapor exchange, several sensitivity tests examined effects of modified parameterizations on tritium transport. These sensitivity tests are discussed later.

Both the tracer vapor exchange and the tracer precipitation parameterizations in the model allow for the isotopic fractionation of tritiated water during all changes of phase. Tritiated water, being heavier than normal water, has a correspondingly lower vapor pressure and molecular diffusivity. Thus, a precipitation droplet will have, after complete equilibration, a higher T/H ratio (i.e., ratio of number of tritium atoms to number of normal hydrogen atoms) than will the surrounding vapor, and surface level HTO will diffuse more slowly toward the ocean surface than will normal water molecules. Jouzel et al. [1987] describe the formulations used for the isotopic fractionation of HDO and $H_2{}^{18}O$ in the GCM. The fractionation of tritium in the present study is treated in the same way, with slightly modified formulas for the equilibrium fractionation factors (H. Craig and B. Lal, The vapor pressure of HTO, unpublished manuscript):

$$\alpha_L = \exp(46480/\theta^2 - 103.87/\theta) \quad (4)$$

$$\alpha_S = \exp(46480/\theta^2 - 103.87/\theta) \quad (5)$$

where α_L is the liquid/vapor fractionation factor, α_S is the solid/vapor fractionation factor, and θ is the temperature in degrees Kelvin. The molecular diffusivity of tritiated water is derived from data available for HDO [Merlivat, 1978] to be 0.968 times that of normal water.

An 8° X 10° horizontal grid was used in the control simulation (simulation 1) and in most of the sensitivity simulations; the ability of the NASA/GISS GCM to simulate realistically the major features of global climate with this horizontal resolution is well documented [Hansen et al., 1983]. The effects of using a finer (4°x5°) grid resolution was examined in simulations 27 and 28. The GCM has a vertical resolution of 9 layers, defined through a σ coordinate; σ has a value of 1 at the surface and 0 at 10-mbar. The model conditions on June 1 of year 3 of the 5-year simulation described by Hansen et al. [1983] were used as the initial conditions for the important atmospheric variables. The simulations (see Table 2) will now be described by discussing the first in detail and then noting the variations imposed in the others.

3.1. Simulation 1: The Standard Case

In simulation 1, the T/H ratio in atmospheric water vapor was initially set everywhere to zero except in a single latitudinal band, where a uniform tritium concentration was imposed. The latitudinal band consisted of 36 grid boxes circling the globe at 51°N and at the 200-mbar level (the seventh GCM level), high in the troposphere. The band was assumed to represent the site of tritium injection from the stratosphere. Since all of the tracer transport processes are completely linear, and since only the relative tritium inputs into the ocean through precipitation and vapor exchange are studied, the magnitude of the imposed T/H ratio is unimportant.

Unfortunately, specific weather events in the model simulation, such as atypically large storms, could transport the initial tritium in a way not consistent with time-averaged transport. To avoid this problem, the T/H ratio in each box of the latitudinal band was reset to its original value at every time step. The original T/H ratio therefore acted as a constant boundary condition at the latitudinal band, and during the first month of simulation, the distribution of tritium in the atmosphere moved toward a "steady state" distribution. The tritium inputs into the ocean were monitored for 30 days, starting on July 1, the beginning of the second month. The 30 July days were assumed to be an adequate averaging period. (July is considered because, as will be discussed later, summer is the important season for tritium deposition in the real world.) As a test of the steady state method, simulation 26 followed tritium transport without resetting the T/H ratios in the source boxes.

Simulation 1 treated the precipitation or condensation of tritium onto nonocean surfaces in a special way. Tritium was not allowed to reevaporate from any earth surface reservoir; the model recorded only where and how the atmospheric tritium first hit the surface. This lessened the required preconditioning period for the simulation. The 30 June days used would have been insufficient if continental groundwater reservoirs had to be properly loaded with tritium. Unfortunately, though, the simulation thereby neglected an important pathway for transporting tritium into the surface layer over the ocean. Tritium could conceivably precipitate onto a continent, reevaporate, and then remain in lower atmospheric levels while advection carries it to sea. The importance of this pathway was investigated in simulation 6, which employed a continental tritium source.

The amounts of tritium entering the ocean as exchanged vapor and as precipitation were determined at every time step of simulation 1. The precipitation and downward vapor flux of model water were also monitored; the latter flux was calculated using equation (2), setting q_g to zero. The 30-day grid square totals for each of these four fluxes were summed over latitudinal bands, with the precipitation fluxes divided into continental and oceanic components.

The results are presented in Table 3. First, the total model water surface fluxes for each band were divided by their respective areas to produce average, per-unit-area fluxes, which appear in the first three columns. Each tritium flux for a band was then divided by the corresponding water flux to obtain an average T/H ratio for that flux.

TABLE 2. Description of Simulations and Ratios of Vapor Impact to Precipitation Delivery of Tritium Into the Oceans

Simulation	Description	Tritium Input Ratio
1	Control: tritium content kept constant in latitudinal band at 51°N and 200 mbar (upper troposphere).	0.79
	Variations in the Tritium Source Location	
2	Tritium source band placed at 100 mbar (lower stratosphere).	0.77
3	Tritium source band placed at 35°N.	0.74
4	Tritium content kept constant in only 2 boxes, over continents.	0.74
5	Tritium content kept constant in only 2 boxes, over oceans.	1.05
6	No atmospheric tritium source; tritium evaporates from continental squares between 30°N and 60°N.	1.60
7	Tritium content kept constant in first layer boxes over pure ocean grid squares north of 30°N.	1.82
8	As 7, but tritium source in level 2 (890 mbar).	1.49
9	As 7, but tritium source in level 3 (790 mbar).	1.06
10	As 7, but tritium source in level 4 (630 mbar).	0.93
11	As 7, but tritium source in level 5 (470 mbar).	0.98
12	As 7, but tritium source in level 6 (320 mbar).	0.98
13	As 7, but tritium source in level 7 (200 mbar).	0.89
14	As 7, but tritium source in level 8 (100 mbar).	0.80
	Variations in Model Physics	
15	Upstream weighting scheme used for dynamical tracer transport.	0.84
16	Tritium in lowest three atmospheric levels vertically mixed.	0.85
17	Drag coefficient in surface flux calculations increased threefold.	1.06
18	Drag coefficient in surface flux calculations divided by 3.	0.47
19	Tritium concentration in surface boundary layer assumed equal to average tritium concentration in first layer grid box.	1.25
20	Total equilibration of falling tritium condensate during moist convection.	0.86
21	No equilibration of falling tritium condensate during moist convection.	0.73
22	Moist convective downdrafts imposed; no equilibration of falling tritium condensate during moist convection.	0.58
23	Fraction of grid box column forming moist convective plume reduced to 1/10.	0.70
24	Tritium condensate formed above 600 mbar set aside and placed in first layer grid box as tritium vapor.	0.77
	Test of Seasonality	
25	Control simulation run under winter (rather than summer) conditions.	0.71
	Variations in Grid Resolution	
27	Control simulation (simulation 1) run with a finer (4°x5°) horizontal grid.	0.98
28	Continental source simulation (simulation 6) run with a finer (4°x5°) horizontal grid.	1.29

Simulations 2-28 are equivalent to simulation 1 except for the changes noted in the simulation description. Keep in mind that Weiss and Roether's [1980] analysis of observational data suggests a tritium input ratio of 2.4.

TABLE 3. Tritium Fluxes as a Function of Latitude for the Tritium Simulations

Median Latitude, °N	30-Day Water Fluxes, kg/m^2			Tritium/Hydrogen With Respect to 51°N Ocean			Tritium Fluxes % of Total in Latitude Range		
	Continental[a] Precipitation	Ocean Precipitation	Ocean Vapor	Continental Precipitation	Ocean Precipitation	Ocean Vapor	Continental Precipitation	Ocean Precipitation	Ocean Vapor
Simulation 1: Upper Troposphere Injection 51°N									
74	41	38	110	1.51	1.10	0.16	6.25	1.39	0.61
66	69	56	119	1.07	0.95	0.15	11.50	2.35	0.76
59	68	55	138	0.86	1.16	0.21	9.17	6.69	3.02
51	80	59	114	0.67	1.00[b]	0.28	9.79	7.87	4.23
43	87	55	151	0.49	0.57	0.20	7.52	6.00	5.87
35	68	86	273	0.26	0.14	0.09	3.06	2.82	5.60
27	68	115	231	0.15	0.03	0.02	1.89	0.84	1.67
20	106	112	258	0.05	0.00	0.01	0.77	-0.01[c]	0.34
Total							49.94	27.96	22.10
Simulation 2: Lower Stratosphere Injection 51°N									
74	41	38	110	2.34	1.54	0.27	8.21	1.65	0.85
66	69	56	119	1.35	1.15	0.19	12.35	2.40	0.85
59	68	55	138	0.93	1.18	0.22	8.45	5.80	2.67
51	80	59	114	0.70	1.00	0.27	8.74	6.66	3.50
43	87	55	151	0.58	0.61	0.20	7.51	5.46	4.96
35	68	86	273	0.34	0.22	0.11	3.43	3.76	6.03
27	68	115	231	0.14	0.07	0.04	1.51	1.85	2.12
20	106	112	258	0.03	0.01	0.01	0.36	0.39	0.50
Total							50.56	27.97	21.47
Simulation 3: Upper Troposphere Injection 35°N									
74	41	38	110	0.62	0.36	0.06	2.29	0.41	0.19
66	69	56	119	0.51	0.40	0.05	4.96	0.89	0.24
59	68	55	138	0.46	0.69	0.12	4.43	3.57	1.51
51	80	59	114	0.51	1.00	0.20	6.75	7.08	2.69
43	87	55	151	0.65	0.91	0.20	9.01	8.59	5.28
35	68	86	273	0.56	0.44	0.14	5.98	8.11	8.55
27	68	115	231	0.30	0.19	0.10	3.28	5.21	5.22
20	106	112	258	0.12	0.05	0.03	1.76	1.51	2.51
Total							38.46	35.36	26.18
Simulation 4: Injection Over Continents 51°N									
74	41	38	110	2.23	1.26	0.21	7.22	1.25	0.62
66	69	56	119	1.59	1.16	0.18	13.48	2.25	0.75
59	68	55	138	1.28	1.42	0.23	10.78	6.43	2.66
51	80	59	114	1.01	1.00	0.27	11.63	6.17	3.21
43	87	55	151	0.79	0.54	0.18	9.59	4.44	4.11
35	68	86	273	0.33	0.14	0.09	3.09	2.28	4.33
27	68	115	231	0.23	0.03	0.02	2.22	0.60	1.27
20	106	112	258	0.08	0.00	0.01	1.01	0.08	0.52
Total							59.02	23.51	17.47

			Simulation 5: Injection Over Oceans 51°N						
74	41	38	110	1.59	1.66	0.26	6.77	2.16	1.01
66	69	56	119	1.06	1.26	0.23	11.74	3.20	1.21
59	68	55	138	0.74	0.99	0.24	8.18	5.88	3.54
51	80	59	114	0.61	1.00	0.34	9.22	8.10	5.32
43	87	55	151	0.30	0.45	0.26	4.68	4.83	7.82
35	68	86	273	0.14	0.11	0.12	1.77	2.27	7.43
27	68	115	231	0.08	0.03	0.03	1.03	0.80	2.06
20	106	112	258	0.04	0.00	0.01	0.71	-0.02[c]	0.28
Total							44.10	27.22	28.68
			Simulation 6: Evaporation From Continents 30°-60°N[d]						
74	41	38	110	1.51	1.54	0.34	5.08	1.66	0.59
66	69	56	119	2.02	1.59	0.36	17.88	2.80	0.87
59	68	55	138	4.25	1.92	0.34	1.26	3.98	2.28
51	80	59	114	4.72	1.00	0.40	1.35	3.23	2.80
43	87	55	151	4.45	1.03	0.24	0.14	1.68	3.23
35	68	86	273	2.91	0.32	0.56	1.53	4.66	16.71
27	68	115	231	0.77	0.16	0.25	7.82	4.02	7.23
20	106	112	258	0.27	0.06	0.10	3.57	1.61	4.03
Total							38.62	23.64	37.74
			Simulation 7: Injection Just Above Ocean 30°N						
74	41	38	110	0.18	0.31	0.15	0.53	0.29	0.41
66	69	56	119	0.15	0.52	0.21	1.18	0.93	0.80
59	68	55	138	0.13	0.58	0.21	0.98	2.45	2.18
51	80	59	114	0.12	1.00	0.50	1.29	5.71	5.48
43	87	55	151	0.11	0.99	0.61	1.23	7.58	12.68
35	68	86	273	0.05	1.01	0.72	0.46	14.87	33.86
27	68	115	231	0.01	0.07	0.12	0.06	1.58	5.14
20	106	112	258	0.01	0.00	0.01	0.07	0.00	0.25
Total							5.80	33.41	60.79
			Simulation 15: Upstream Weighting for Tracer Transport[e]						
74	40	44	108	1.57	1.34	0.23	4.29	1.34	0.56
66	65	57	144	1.28	1.26	0.17	8.79	2.15	0.71
59	65	57	137	1.10	1.09	0.18	7.56	4.41	1.78
51	91	49	102	0.92	1.00	0.26	10.43	4.40	2.38
43	93	64	149	0.69	0.69	0.24	7.65	5.73	4.67
35	75	79	249	0.42	0.36	0.15	3.75	4.58	6.12
27	69	105	224	0.32	0.19	0.10	2.70	3.55	4.22
20	98	120	239	0.19	0.10	0.07	1.86	2.64	3.71
Total							47.04	28.80	24.16
			Simulation 16: Tritium Mixed in Lowest Three Layers[e]						
74	40	44	108	1.18	0.79	0.16	5.37	1.31	0.64
66	65	57	144	0.98	0.92	0.13	11.21	2.62	0.92
59	65	57	137	0.79	0.94	0.20	9.03	6.33	3.16
51	91	49	102	0.58	1.00	0.33	10.92	7.30	5.00
43	93	64	149	0.37	0.53	0.22	6.81	7.24	7.08
35	75	79	249	0.14	0.14	0.08	2.09	2.93	5.03
27	69	105	224	0.11	0.02	0.03	1.50	0.58	1.90
20	98	120	239	0.02	0.01	0.01	0.28	0.26	0.49
Total							47.20	28.58	24.22

TABLE 3. (continued)

Median Latitude, °N	30-Day Water Fluxes, kg/m^2			Tritium/Hydrogen With Respect to 51°N Ocean			Tritium Fluxes % of Total in Latitude Range		
	Continental[a] Precipitation	Ocean Precipitation	Ocean Vapor	Continental Precipitation	Ocean Precipitation	Ocean Vapor	Continental Precipitation	Ocean Precipitation	Ocean Vapor
Simulation 17: Drag Coefficient Increased 3 Times									
74	42	65	406	1.89	1.01	0.12	4.98	1.38	0.99
66	83	77	411	1.68	1.60	0.12	13.40	3.34	1.30
59	94	74	180	1.26	1.67	0.33	11.51	7.98	3.77
51	95	65	269	0.77	1.00	0.19	8.31	5.33	4.28
43	90	79	405	0.64	0.47	0.17	6.28	4.36	8.14
35	90	105	590	0.24	0.18	0.09	2.32	2.77	7.24
27	92	122	489	0.10	0.00	0.01	1.07	0.09	0.93
20	186	157	598	0.01	0.00	0.00	0.16	-0.08[c]	0.15
Total							48.03	25.18	26.79
Simulation 18: Drag Coefficient Divided by 3									
74	45	42	55	1.50	1.19	0.22	7.42	1.83	0.46
66	59	40	85	1.25	1.03	0.14	12.45	1.97	0.56
59	63	54	46	0.93	1.13	0.28	9.92	6.95	1.55
51	68	48	66	0.63	1.00	0.26	8.53	6.89	2.48
43	80	58	70	0.47	0.71	0.21	7.12	8.42	3.10
35	95	64	97	0.24	0.21	0.14	4.39	3.48	3.42
27	42	87	118	0.20	0.06	0.06	1.61	1.57	2.02
20	114	88	86	0.07	0.03	0.05	1.39	0.97	1.51
Total							52.82	32.09	15.09
Simulation 19: Tritium Mixed Into Surface Boundary Layer									
74	41	38	110	1.61	1.12	0.33	5.63	1.20	1.04
66	69	56	119	1.13	0.92	0.36	10.26	1.92	1.60
59	68	55	138	0.93	1.12	0.45	8.38	5.50	5.57
51	80	59	114	0.73	1.00	0.47	9.09	6.65	6.01
43	87	55	151	0.55	0.60	0.33	7.12	5.29	8.06
35	68	86	273	0.29	0.15	0.12	2.89	2.63	6.41
27	68	115	231	0.16	0.04	0.03	1.63	0.92	1.47
20	106	112	258	0.05	0.00	0.00	0.62	0.10	0.01
Total							45.62	24.20	30.18
Simulation 20: Total Equilibration in Moist Convection									
74	41	38	110	1.60	1.15	0.18	6.24	1.37	0.63
66	69	56	119	1.14	1.00	0.16	11.65	2.33	0.78
59	68	55	138	0.91	1.21	0.23	9.25	6.64	3.11
51	80	59	114	0.72	1.00	0.31	9.97	7.43	4.36
43	87	55	151	0.52	0.55	0.22	7.62	5.43	6.08
35	68	86	273	0.28	0.14	0.09	3.09	2.66	5.82
27	68	115	231	0.16	0.03	0.03	1.89	0.81	1.73
20	106	112	258	0.05	0.00	0.01	0.77	0.00	0.33
Total							50.49	26.68	22.83

			Simulation 21: No Equilibration in Moist Convection						
74	41	38	110	1.37	1.03	0.14	6.49	1.50	0.60
66	69	56	119	0.91	0.86	0.13	11.26	2.44	0.77
59	68	55	138	0.72	1.01	0.17	8.84	6.74	2.92
51	80	59	114	0.53	1.00	0.23	8.95	9.04	4.05
43	87	55	151	0.40	0.61	0.17	7.06	7.34	5.71
35	68	86	273	0.21	0.11	0.08	2.89	2.47	5.78
27	68	115	231	0.12	0.02	0.02	1.76	0.53	1.80
20	106	112	258	0.04	0.00	0.01	0.65	0.03	0.38
Total							47.89	30.09	22.02
			Simulation 22: Downdrafts in Moist Convection						
74	48	40	86	1.29	1.01	0.17	5.36	1.17	0.39
66	63	55	131	1.34	0.94	0.10	11.19	1.93	0.49
59	74	66	140	1.41	1.20	0.14	13.77	6.98	1.83
51	75	59	120	1.17	1.00	0.19	13.81	6.68	2.46
43	66	50	162	0.65	0.52	0.15	6.44	4.23	3.94
35	127	87	244	0.31	0.23	0.07	5.92	3.97	3.45
27	71	63	326	0.23	0.02	0.02	2.49	0.26	1.32
20	130	63	340	0.05	0.01	0.01	0.88	0.25	0.80
Total							59.86	25.47	14.67
			Simulation 23: Moist Convective Plume Size Reduced						
74	41	37	96	1.59	1.05	0.18	7.47	1.46	0.62
66	52	54	98	1.05	0.86	0.14	9.62	2.29	0.71
59	66	64	176	0.82	1.15	0.14	9.44	8.67	2.90
51	74	62	140	0.51	1.00	0.21	7.83	9.19	4.36
43	83	48	174	0.39	0.52	0.15	6.45	5.30	5.43
35	100	92	338	0.19	0.16	0.07	3.77	3.80	5.81
27	61	102	239	0.12	0.02	0.02	1.50	0.51	1.45
20	108	106	258	0.04	0.00	0.01	0.68	0.17	0.58
Total							46.76	31.38	21.86
			Simulation 24: Spurious Precipitation Formed Above 600 mbar Removed[e]						
74	40	44	108	1.02	0.73	0.14	4.61	1.22	0.58
66	65	57	144	0.94	0.85	0.12	10.74	2.40	0.85
59	65	57	137	0.77	0.87	0.18	8.77	5.83	2.96
51	91	49	102	0.62	1.00	0.33	11.61	7.30	4.93
43	93	64	149	0.37	0.64	0.21	6.86	8.81	6.70
35	75	79	249	0.16	0.18	0.08	2.35	3.85	5.45
27	69	105	224	0.10	0.02	0.02	1.36	0.59	1.33
20	98	120	239	0.02	0.00	0.01	0.29	0.19	0.44
Total							46.58	30.18	23.24

TABLE 3. (continued)

Median Latitude, °N	30-Day Water Fluxes, kg/m^2			Tritium/Hydrogen With Respect to 51°N Ocean			Tritium Fluxes % of Total in Latitude Range		
	Continental[a] Precipitation	Ocean Precipitation	Ocean Vapor	Continental Precipitation	Ocean Precipitation	Ocean Vapor	Continental Precipitation	Ocean Precipitation	Ocean Vapor
				Simulation 25: Control Run Under Winter Conditions					
74	34	104	0	3.54	1.63	-	6.74	1.40	0.53
66	40	123	206	3.42	1.43	0.40	11.29	2.26	1.07
59	39	98	151	3.48	1.51	0.39	10.92	6.35	2.58
51	40	102	181	3.47	1.00	0.28	12.31	6.36	3.08
43	56	113	216	1.60	0.58	0.19	7.56	5.96	3.76
35	81	108	294	0.94	0.20	0.11	6.35	2.46	3.66
27	63	93	365	0.16	0.07	0.06	0.89	0.82	2.49
20	53	115	402	0.06	0.00	0.01	0.23	0.03	0.92
Total							56.27	25.63	18.09

[a]"Continental" precipitation includes precipitation onto ocean ice.

[b]For purposes of presentation, the T/H ratios in the various water fluxes were scaled so that the T/H ratio in ocean precipitation at 51°N is 1.00. This is done for each simulation. For simulation 1, the T/H ratio in ocean precipitation at 51°N is actually 0.00184 times that in the atmospheric tritium source.

[c]The slopes scheme for calculating advective transports of tritium occasionally produces small "negative tracer masses." To prevent this, negative masses could be zeroed as they occur; this, however, would violate mass conservation. Alternatively, advective transport of tritium could be limited to prevent the formation of negative masses, but this would result in artificially increased tritium diffusion. It was thought best to allow the small negative tritium masses to exist. The "negative precipitations" formed at steady state are always of negligible magnitude.

[d]The tritium fluxes in the final three columns for simulation 6 do not include the fluxes onto the evaporative source itself. The calculation of the T/H ratio in ocean vapor (sixth column) for simulation 6 also disregarded the vapor over ocean portions of evaporative source squares.

[e]The water fluxes in simulations 15, 16, and 24 are slightly different from those in simulation 1, even though the imposed changes in these simulations affected only tritium transport. The changes in the water fluxes are due to minor changes in the computer system between simulations and should not affect the inherent model climate or the resulting tritium input ratio.

These ratios, meaningful only in their relative values, appear in the next three columns. Finally, the total tritium fluxes are listed in the last three columns, expressed in percent of the total tritium deposition between 16°N and 80°N. (This is the latitude range examined in each simulation. In each simulation, nearly all of the tritium was deposited in this range.)

The last three columns of Table 3 were summed to determine the global relative inputs of tritium onto the continents and oceans. In simulation 1, 28.0% of the tritium entered the ocean as precipitation, while only 22.1% entered as exchanged vapor. The rest precipitated onto the continents. Thus, the ratio of the vapor exchange input of tritium into the ocean to the precipitation input was 0.79, quite different from the ratio of 2.4 proposed by Weiss and Roether [1980]. This difference, in fact, is the essential point of this paper. The ratio of 0.79 for simulation 1 is listed in Table 2 along with the corresponding ratios determined in the other simulations.

To get a rough idea of the interannual variability inherent in the standard tracer model, simulation 1 was repeated twice, using as initial conditions the model conditions on June 1 of years 2 and 4 of the 5-year simulation described by Hansen et al. [1983]. The resulting ratio of the total tritium input into the ocean via vapor exchange to that via precipitation, hereafter referred to as the tritium input ratio, was 0.81 in one simulation and 0.69 in the other. Thus, in the sensitivity simulations described below, variations of the tritium input ratio of the order of 0.1 should not be considered especially significant. The initial conditions that produced the tritium input ratio of 0.79 for the standard model were used in the sensitivity simulations below.

3.2. Simulations 2 - 14: Variation in the Tritium Source Location

In simulation 2, the latitudinal band representing the tritium source remained at 51°N but was displaced one grid box level upward, so that it was vertically centered at 100 mbar (i.e., in the lower stratosphere). The simulation was otherwise equivalent to simulation 1. The resulting tritium input ratio was 0.77. Apparently, moving the tritium source vertically into the stratosphere has little effect on the relative importance of the tritium delivery mechanisms. As shown in Table 3, neither does it significantly affect the geographic distribution of the delivery.

The latitudinal band for tritium injection was displaced southward in simulation 3, placing the tritium source at 35°N and 200 mbar. Although this did displace southward the location of maximum tritium inputs into the ocean (see Table 3), the effect on the tritium input ratio was slight, the new value being 0.74.

Simulations 4 and 5 investigated the effects of a more localized release of tritium. The tritium source for simulation 4 was not a latitudinal band but two single grid boxes lying over North America and Eurasia. The tritium source in simulation 5 also consisted of two single grid boxes, but these boxes were located over the Atlantic and Pacific oceans. As in the other simulations, the T/H ratios in the source boxes were initialized to a given value and reset to that value at every time step. The resulting tritium input ratios for simulations 4 and 5 were 0.74 and 1.05, respectively. The longitudinal position of the tritium source clearly has an effect on the tritium input ratio. The effect is not large enough, however, to make the model ratio consistent with the Weiss and Roether ratio.

As mentioned before, simulation 6 examined one possible pathway for moving high-level tritium into lower levels over the ocean, namely by advection over the sea of tritium that initially precipitates onto continents and subsequently reevaporates. The atmosphere was assumed completely free of tritium at the beginning of the simulation, and none of the tritium sources utilized above were defined for the atmosphere. Instead, tritium was allowed to "evaporate" from continental grid squares between 31°N and 63°N. That is, the first layer grid box above each of these continental grid squares was injected at every time step with an amount of tritium proportional to the model water evaporation from that square. The simulation was otherwise equivalent to the previous simulations. The resulting tritium input ratio was a relatively large 1.60. Thus tritium evaporated from continental reservoirs appears to remain in lower atmospheric levels as it moves out to sea.

If simulation 1 had accounted for the reevaporation of tritium from continents, one might expect that the reevaporated tritium would have entered the oceans as indicated by simulation 6. Consider that in simulation 1, as shown in Table 3, 50% of the tritium released from the upper troposphere source first precipitated onto nonocean surfaces, while the rest entered the ocean directly. Consider also that at the time of the GEOSECS observational survey (see Broecker et al. [1986] for summary), 70% of continental tritium had reevaporated and had advected out over the oceans, 15% had been incorporated into continental runoff, and 15% had remained on the continents. Thus, for every 50 units of tritium that enter the ocean via precipitation or vapor exchange directly, i.e., without reaching the continental surface first, perhaps 35 units of reevaporated continental tritium enter the ocean via these same processes. This would lead to an average tritium input ratio of $(0.79)(50/85) + (1.60)(35/85)$, or 1.1.

In fact, Weiss and Roether [1980] assumed that tritium vapor advected off continents is removed by coastal waters within about 1000 km from shore. They even computed this continental input separately. If their assumption is correct, their observed ratio of 2.4 should be compared to the control simulation ratio of 0.79 alone, since continental reevaporation played no role in this simulation. Some, however [e.g., Ehhalt, 1971], believe that ocean vapor tritium concentrations, even in mid-ocean, are controlled in part by tritium advected off continents. If this is true, Weiss and Roether's ratio of 2.4 inherently accounts for the continental input and should be compared to the effective GCM ratio of 1.1. In either case, the tritium input ratio generated by the GCM is substantially less than that implied by the observations.

Simulation 7 moved the atmospheric tritium source to just above the ocean surface; the first layer grid box above each pure ocean grid square north of 30°N was defined as a source for tritium and was maintained at a constant T/H ratio. As this is certainly not a realistic representation of a bomb tritium source, the high (1.82) tritium input ratio generated in this simulation does not reflect conditions in the real world. Rather, simulation 7 tested the importance of moving tritium vapor to surface levels before it precipitates. It suggests that if the GCM transported high-level tritium to lower levels more efficiently, its delivery of tritium to the ocean might move closer to the Weiss and Roether scenario.

Studied together, simulations 7 through 14 describe more completely the response of the tritium input ratio to the source layer height. Simulation 8 used the same horizontal distribution of source boxes as did simulation 7, but all source boxes were located in the second atmospheric layer (890 mbar). In simulation 9, the same horizontal source box distribution was placed in the third atmospheric layer (790 mbar), and so on through the eighth layer. The results, listed in Table 2, show an essentially steady decrease in tritium input ratio with an increase in source height. Each atmospheric level seems to provide some resistance to the transport of tritium vapor from the source to the ocean surface.

3.3. Simulations 15 - 24: Variation in Model Physics

The simulations in this section, each featuring a single change in some model parameterization, used the same tritium source and the same model initial conditions as used in simulation 1. The resulting tritium input ratios should be compared to the simulation 1 value of 0.79.

3.3.1. Changes in the dynamical transport of tritium vapor. To increase the model's tritium input ratio, the relative importance of tritium vapor exchange at the ocean surface must increase. Two simulations attempted to move more tritium vapor from the seventh layer source to the ocean surface by modifying the tracer advection scheme.

The slopes scheme of Russell and Lerner [1981] is the standard scheme used for transporting tracers; as described by Jouzel et al. [1987], the gradient of tracer concentration in water within every grid box is stored and updated at every time step with this scheme, and the resulting information on subgrid tracer distribution helps produce a more reasonable estimate of the tracer transported between adjacent boxes. The slopes scheme was replaced by an upstream weighting scheme in simulation 15. Tritium transport was calculated in this simulation by assuming that the average T/H ratio for a given grid box applied everywhere within the box and thus within any water vapor transported out of the box. The scheme is inherently more diffusive and was therefore expected to ease the vertical transport of tritium vapor to the ocean surface. Simulation 15, however, produced a tritium input ratio of only 0.84.

Simulation 16 attempted to ease the downward transport of tritium vapor by maximizing vertical mixing in the lowest three atmospheric layers. At every time step in this simulation, the tritium (but not the water vapor) in the lowest three boxes of every vertical column was redistributed so as to produce the same T/H ratio in each box while conserving tritium mass. This seemingly arbitrary mixing was suggested by certain vertical tritium profile measurements that show the T/H ratio in vapor to be roughly uniform in the first 2 km above the Earth's surface [Ehhalt, 1971; Taylor, 1972]. As in the previous simulations, the tritium specific humidity at the top of the surface boundary layer (q_{st} in equation (3)) was lower than the average specific humidity in the lowest grid box due to dilution by evaporating tritium-free ocean water. The added mixing in the lowest three boxes did not substantially increase the tritium input ratio; it raised it only slightly to 0.85.

3.3.2. Changes in the parameterization of surface vapor exchange. The sensitivity of the tritium input ratio to the surface vapor exchange parameterization was tested first by varying the transfer coefficient C_q in equations (2) and (3); the best value to use for this parameter has never been known with certainty. The value of C_q was increased threefold in simulation 17 and was decreased threefold in simulation 18. The resulting global evaporation of water was increased by only 20% in simulation 17 and was decreased by only 20% in simulation 18; apparently each change in the transfer coefficient was counterbalanced by an opposing change in the average vapor deficit ($q_g - q_s$) in equation (2). The resulting tritium input ratios were 1.06 for simulation 17 and 0.47 for simulation 18. The simulation 17 ratio was still far from the Weiss and Roether ratio of 2.4. The increase in the transfer coefficient must have eased tritium transport across the ocean surface, but depleted first layer tritium was apparently not replenished rapidly enough by tritium from higher layers.

The parameterization of downward tritium vapor flux across the ocean surface is quite crude. Equation (2) was developed to estimate net water evaporation only; interpreting the two terms in the expanded equation as an upward and downward flux, and thereby producing equation (3) by analogy for the downward flux of tritium, is arguably inappropriate. It is reasonable to assume, however, that the downward flux of tritium vapor into the ocean is proportional to the tritium content of the first layer grid box. The sensitivity of the results to a large change in the proportionality constant is effectively examined in simulations 17 and 18.

Simulation 19 attempted to increase the surface vapor exchange of tritium by calculating q_{st} in equation (3) as

$$q_{st} = q_s \left(\frac{q_{1t}}{q_1}\right) \qquad (6)$$

where q_{1t}/q_1 represents the average T/H ratio in the first layer grid box. Simulation 19 thus assumed this average T/H ratio to apply at the top of the surface boundary layer. Although the modifications in tritium transport introduced in simulations 17 and 19 can be shown to be qualitatively equivalent, simulation 19 is considered separately because it left the transport of water vapor unchanged. The tritium input ratio for simulation 19 was 1.25, again suggesting some difficulty in

moving tritium from higher to lower atmospheric layers in the GCM.

Although the tritium input ratios produced in simulations 17 and 19 are not large enough to be consistent with the Weiss and Roether result, they do seem significantly larger than that of the control simulation. The tritium input ratio seems more sensitive to the parameterization of vapor exchange than to the tested modifications in tritium advective transport and (as shown below) precipitation removal. Note that if the vapor exchange parameterization was similarly changed in the continental source simulation (simulation 6), its resulting tritium input ratio might be similarly increased.

3.3.3. Changes in the parameterization of precipitation. If the vapor exchange input of tritium into the ocean is not too small in the model, then perhaps the precipitation input of tritium is too large. Also, perhaps the precipitation processes can be made more efficient at loading the lower atmospheric layers with tritium vapor. The following sensitivity studies address these hypotheses.

One mechanism for moving tritium vapor into lower atmospheric layers involves the equilibration of falling liquid condensate. Precipitation droplets forming from the tritium-rich vapor in upper layers become enriched with tritium themselves. As they fall into lower layers, they equilibrate with vapor relatively deficient in tritium, resulting in a net transfer of tritium out of the droplets.

The efficiency of this lower-layer tritium loading is naturally dependent on the extent of equilibration. The previous simulations allowed falling liquid condensate to equilibrate completely with surrounding vapor during large-scale condensation events, since these events in nature are associated with small droplets having isotopic relaxation times of the order of a few seconds [Jouzel et al., 1975]. In contrast, the larger droplets associated with moist convective events have relaxation times of up to a few minutes and can never reach isotopic equilibrium. This was demonstrated by Federer et al. [1982] with a convective cloud model developed for stable isotopes. The extent of equilibration during moist convection for the unstable isotope tritium has not been documented, so the extent was chosen arbitrarily in simulations 1 through 19 above. During moist convective events, only half the falling condensate was allowed to equilibrate with surrounding vapor. Recall that the surrounding vapor itself is only a portion of the total grid box vapor.

The effect of the extent of equilibration on the tritium input ratio was investigated in simulations 20 and 21. In simulation 20, all of the falling liquid condensate in a moist convective event equilibrated with the surrounding vapor, and in simulation 21, none of it did. The resulting tritium input ratios for simulations 20 and 21 were 0.86 and 0.73, respectively; recall that simulation 1 yielded a ratio of 0.79. An increase in the extent of equilibration does produce an increase in the tritium input ratio. When considered, however, against the aforementioned interannual variability in simulations with the standard model, the increase is not significant.

Moist convective downdrafts, which are not currently modeled in the GCM, constitute another mechanism for moving high-level tritium into layers nearer the surface. In the standard model, when a moist convective plume forms and lifts an air mass from layer A into a higher layer B, the air mass deficit in layer A is filled by letting the air outside the plume gently subside. Simulation 22 tested the importance of the downdraft mechanism by replacing subsidence with a more direct downward transport of air. After the rise of the plume in simulation 22, an equivalent air mass was removed from layer B and directly inserted into layer A without affecting the layers in between. If tritium existed in layer B, an appropriate portion was also transported downward. The structure of the moist convection algorithm made it necessary in this simulation to prevent equilibration of tritium in falling raindrops with tritium in surrounding vapor, as in simulation 21. The complete replacement of subsidence by downdrafts is by all means an extreme, and the resulting tritium input ratio of 0.58 indicates that downdrafts as modeled do not increase the relative importance of tritium vapor exchange at the ocean surface.

The results of simulation 22 are counterintuitive; the moist convective downdrafts were expected to increase the tritium input ratio rather than lower it. An examination of the simulation data shows, however, that the extreme parameterization change had an important effect on model climate, reducing precipitation in the tropics and modifying the distribution of the mass stream function. The change also reduced the average depth of moist convection in the model. The lower tritium input ratio in simulation 22 may be quite consistent with the new, less accurate model climate. Due to these climate changes, the simulation is an inconclusive test of the importance of the downdraft mechanism. Still, even in a poor climate, one would expect the tritium input ratio in simulation 22 to have increased substantially if the lack of downdrafts were indeed the main reason for the model's inconsistency with the Weiss and Roether result.

In simulation 23, the fraction of an unstable grid box that becomes a moist convective plume, arbitrarily chosen to be one-half in the previous simulations, was changed to one-tenth. The grid box fractions used in the condensate reevaporation and equilibration calculations were correspondingly reduced. The resulting monthly global precipitation for simulation 23 differed only slightly from that of simulation 1; apparently the reductions in hourly moist convective precipitation over a grid square were counterbalanced by an increased precipitation frequency, since instabilities in the air column were removed less efficiently. The modified parameterization and any associated changes in precipitation frequency also had only a small effect on the tritium input ratio, producing a value of 0.70.

Simulation 24 examined the possibility that the model-produced tritium input ratio is lower than the ratio suggested by Weiss and Roether due to the formation of spurious precipitation in the model's upper troposphere. The moisture holding capacity of air is much greater in the lower atmospheric layers of the model, where temperatures are higher; thus most of the GCM's water vapor resides in these layers, and these layers naturally produce most of the GCM's precipitation. Precipi-

tation amounts formed in the colder higher layers are necessarily small and thus can be quite inaccurate without greatly affecting the GCM's surface precipitation fields. When coupled, however, with the relatively large T/H ratios in higher layers (see section 4.1 and Figure 1), spurious precipitation formed in higher layers could contain significant amounts of tritium. This tritium precipitation would also be spurious.

In simulation 24, tritium contained in precipitation falling into the fourth vertical layer (centered at 630 mbar) was removed from the precipitation and set aside. Once the precipitation reached the Earth's surface, this tritium was inserted into the lowest atmospheric layer as tritium vapor. Therefore, spurious tritium condensate formed above layer 4 was given ample opportunity to enter the ocean as exchanged vapor. The tritium input ratio for this run was 0.77, roughly the same as that for the standard run. Spurious precipitation in higher layers, if it exists, does not seem to enhance much the precipitation of tritium at the ocean surface.

3.4. Simulation 25: Test of Seasonality

If the importance of a tritium transport mechanism varies with season, so might the value of the tritium input ratio. To test this, simulation 1 was repeated under winter conditions as simulation 25. The model's prognostic variables were initialized using the model conditions on December 1 of year 2 of the 5-year simulation described by Hansen et al. [1983]. Tritium fluxes across the ocean surface were monitored over a 30-day period starting on January 1. The resulting tritium input ratio of 0.71 is actually less than the value of 0.79 found for summer.

3.5. Simulation 26: Transient Case

The above simulations maintained the tritium source boxes at a constant T/H ratio and allowed the atmospheric distribution of tritium to approach steady state before monitoring the tritium fluxes at the ocean surface. Again, this was to produce a tritium input ratio based on monthly averaged weather conditions and not on a few specific and possibly singular weather events. Simulation 26 checked the validity of this approach by monitoring the transient behavior of a single impulse of tritium released at the beginning of the simulation. One unit of tritium was placed in one grid box in the lower stratosphere (100 mbar; model layer 8), directly above an important Soviet nuclear testing site in northern Siberia (at 75°N, 55°E). Tritium leaving the box was never restored; thus the sum of the total tritium contained in the atmosphere and the cumulative total downward tritium flux at the Earth's surface remained constant.

Simulation 26 followed the tritium transport for 13 weeks, starting on June 1. The tritium input ratio and total amount of tritium removed (in percent) for each week are tabulated in Table 4; notice that in the transient regime, as in the steady state regime, the ratio is never close to the ratio of 2.4 suggested by Weiss and Roether. The weighted average tritium input ratio over the first 13 weeks is 0.68. The time scale for tritium removal indicated in Table 4 is higher than that for the simulations above because simulation 26 used a stratospheric tritium source.

TABLE 4. Tritium Input Ratios as a Function of Time for Simulation 26

Week	Tritium Input Ratio	Amount of Initial Tritium Removed During Week, %
1	0.39†	3.7
2	0.17†	4.3
3	0.75†	7.8
4	0.74	8.7
5	0.71	8.4
6	0.58	7.9
7	0.61	6.6
8	0.76	6.4
9	0.74	5.8
10	0.78	5.2
11	0.90	3.6
12	0.80	3.6
13	0.77	3.1
Total removed		75.0

In simulation 26, an impulse of tritium was released in the stratosphere at the beginning of the first week. The tritium input ratios are determined from precipitation and vapor exchange inputs into the ocean averaged over each listed week.

†The first tritium input ratios listed might be considered spurious; at the beginning of this transient simulation, large tritium concentration gradients produced "negative tritium masses" (see third footnote, Table 3) that led to questionable tritium surface fluxes during the first three weeks. The surface fluxes after three weeks were not similarly affected, since by this time the concentration gradients were greatly reduced. Note that this problem did not influence the tritium input ratios generated in the other simulations, since the surface fluxes in the other simulations were monitored only after the distribution of atmospheric tritium reached steady state.

3.6. Simulations 27 and 28: Effect of Model Resolution

All of the GCM simulations above used an 8°x10° horizontal grid. The GISS GCM was specifically designed to simulate major climate characteristics well with this grid spacing. Still, certain features of atmospheric transport change (often improve) when this GCM is run with a finer (4°x5°) grid, and some of these changes may affect tritium transport. With the finer grid, it is possible to represent frontal vertical motions better, and vertical motions associated with the Ferrel cell are stronger [Rind, 1988]. Furthermore, penetrating convection is enhanced [Rind, 1988]. Implicit horizontal tracer diffusion is also reduced, since advected water vapor is effectively spread over a smaller grid box area.

To determine the effects of grid resolution on the model results, the control simulation (simulation 1) and the simulation using the continental tritium source (simulation 6) were repeated with

the 4°x5° horizontal grid as simulations 27 and 28, respectively. Archived data from a long-term 4°x5° GISS GCM simulation provided the appropriate June 1 initial conditions. Simulation 27 produced a tritium input ratio of 0.98 (compared to 0.79 for simulation 1), while simulation 28 produced a ratio of 1.29 (compared to 1.60 for simulation 6).

These results are easily explained. Apparently, the increased vertical motion in the finer grid led to a more efficient downward transport of high-altitude tritium vapor in simulation 27, leading to a relatively higher vapor exchange input of tritium into the ocean. In simulation 28, increased vertical transport and decreased horizontal transport of tritium released from the continents apparently led to relatively higher tritium concentrations in upper levels over the ocean and thus to a stronger relative precipitation input.

The effective tritium input ratio for the finer grid model can be determined from the results of simulations 27 and 28. In simulation 27, 54% of the tritium released from the upper troposphere precipitated onto nonocean surfaces. As in the discussion of simulation 6 above, it is assumed that 70% of this tritium reevaporates and enters the ocean via precipitation or vapor exchange. The weighted average tritium input ratio, accounting for both the direct and continental pathways into the ocean, is then 1.1. This is the same as the ratio computed from the results of simulations 1 and 6; thus, in this one sense, the effect of the finer grid on the transport of reevaporated continental tritium counteracts its effect on the transport of upper tropospheric tritium.

4. Discussion

4.1. Vertical T/H Profiles

With the main tritium source in the upper troposphere and a tritium sink and water source at the Earth's surface, an equilibrium vertical profile for tritium might be characterized by an increase in T/H ratio with height. Ehhalt [1971] observed this profile structure over Scottsbluff, Nebraska. The average profile (derived from 12 measured profiles) over Scottsbluff for the period between February 10 and June 21, 1966, is reproduced in Figure 1. Ehhalt suggests some possible reasons for the small increase in T/H ratio at ground level, including local reevaporation of tritium and the short-term presence of two different air masses, the lower one consisting of polar air loaded with tritium due to an extended residence time over the continent. Note that since evaporation of tritium from the ground surface is prevented in the control simulation of the tracer model, these processes cannot similarly affect the control simulation's vertical T/H profiles.

The model-generated vertical profiles of T/H ratio over the grid square containing Scottsbluff and over a grid square in the Atlantic Ocean are also shown in Figure 1. These profiles were constructed from simulation 1 (the control simulation) data as follows. The average monthly tritium content for each grid box in a column was divided by the average monthly water content for the box. Then, the resulting profile was scaled so that it matched the observed profile exactly at a height of 6 km. (Due to the arbitrary source box concentration, only relative tritium quantities in the model atmosphere have meaning; therefore, only the vertical gradients of relative tritium concentration are being compared in Figure 1.) The observed and modeled gradients agree quite well.

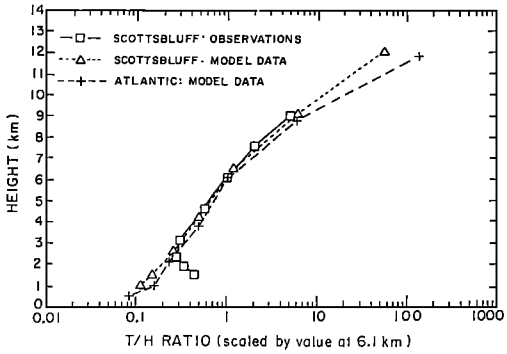

Fig. 1. Observed and model-generated vertical profiles of the T/H ratio. Observations were taken above Nebraska and span the period February 10 to June 21, 1966 [Ehhalt, 1971]. One of the model-generated profiles lies over the grid square containing Nebraska, and the other lies over the North Atlantic (30°W, 43°N). For comparison purposes, all T/H ratios in a given profile were divided by the profile value at 6.1 km.

4.2. Comparison With the Weiss and Roether Ratio

The model results indicate a strong insensitivity of the tritium input ratio to the location of the tritium source and to the parameterizations of the model physics. Perhaps the best estimate of the model-generated tritium input ratio is 1.1, based on the ratio of 0.79 for the standard simulation (simulation 1), the ratio of 1.6 for the continental tritium source simulation (simulation 6), and an estimate of the amount of real-world tritium that evaporated off the continents before entering the ocean. (See the discussion of simulation 6 above.) The simulations that used the finer (4°x5°) grid (simulations 27 and 28) together produced the same effective ratio. This ratio of 1.1 is less than half that obtained by Weiss and Roether [1980].

An obvious explanation for the discrepancy is that the model is unable to simulate properly the transport of tritium in the atmosphere. The sensitivity tests discussed above are extensive but perhaps not complete; the model may still fail to simulate an important pathway for moving tritium to the ocean surface. Accounting for the small concentration of tritium in ocean surface water might increase the GCM-generated tritium input ratio, but only slightly.

Problems may have arisen from limitations imposed on vertical transport by model resolution. An 8°x10° model cannot properly resolve, for example, baroclinic fronts and downward motions during moist convection. Perhaps these resolution problems also influenced, though to a lesser extent, the results of simulations 27 and 28, which used a 4°x5° grid. The agreement shown in Figure 1 between the model-generated and observed tritium concentration profiles does, however, support the model's ability to transport tritium vertically.

TABLE 5. Summary of the T/H Data Obtained by Weiss and Roether [1980] From Measurements on Rain/Vapor Pairs

Date	Latitude	Longitude	T/H Rain, TU†	T/H Vapor TU	T/H Vapor / T/H Rain	T/H Rain / T/H Vapor
Aug. 1-3, 1966	57° to 59°N	8° to 3°W	442	242	0.55	1.82
Aug. 4-6, 1966	59° to 63°N	3° to 23°W	598	286	0.48	2.08
Aug. 10-14, 1966	63°N	24° to 40°W	188	248	1.32	0.76
Aug. 15-19, 1966	63° to 62°N	18° to 40°W	205	204	1.00	1.00
Aug. 20-24, 1966	62° to 61°N	40° to 41°W	197	158	0.80	1.25
Aug. 25-29, 1966	61° to 59°N	41° to 43°W	142	129	0.91	1.10
Aug. 30 to Sept. 3, 1966	59° to 61°N	43° to 28°W	(48)?	124	(2.58)?	(0.39)?
Sept. 4-8, 1966	61° to 62°N	28° to 8°W	222	155	0.70	1.43
Sept. 11-13, 1966	62° to 54°N	7°W to 8°E	190	95	0.50	2.00
Mean					0.78	1.43 (8)
Sept. 27 to Oct. 2, 1966	51° to 37°N	1°E to 8°W	98	76	0.77	1.30
Oct. 2-7, 1966	37° to 43°N	8°W to 8°E	98	79	0.81	1.23
Oct. 10-15, 1966	43°N	8° to 7°E	137	79	0.58	1.72
Oct. 17-22, 1966	44°N	8°E	46	67	1.46	0.68
Oct. 24-29, 1966	44° to 43°N	8° to 7°E	89	58	0.65	1.54
Oct. 31 to Nov. 4, 1966	44° to 36°N	7° to 8°E	40	70	1.75	0.57
Nov. 9-11, 1966	36° to 50°N	8° to 3°E	66	74	1.13	0.88
Mean					1.02	1.13 (7)
Jan. 18-22, 1967	38° to 35°N	11° to 7°W	44	30	0.69	1.45
Jan. 30 to Feb. 4, 1967	34° to 37°N	9°W	124	61	0.50	2.00
Feb. 5-9, 1967	37°N	9°W	92	58	0.63	1.59
Feb. 12-17, 1967	37°N	10°W	74	58	0.78	1.28
Feb. 18-22, 1967	37°N	10°W	29	20	0.69	1.45
Feb. 23-27, 1967	37° to 36°N	10° to 6°W	62	34	0.55	1.82
Mean					0.64	1.60 (6)
April 15-20, 1967	30°N	28° to 29°W	87	40	0.46	2.17
April 20 to May 4, 1967	30° to 29°N	29° to 25°W	69	57	0.83	1.21
May 22-26, 1967	28°N	18° to 16°W	96	41	0.42	2.38
June 1-5, 1967	30° to 29°N	28° to 29°W	44	40	0.91	1.10
Mean					0.66	1.72 (4)
July 13-18, 1968	62° to 63°N	9°W	157	95	0.60	1.67
July 19-23, 1968	63° to 62°N	9° to 12°W	96	53	0.55	1.82
July 26-31, 1968	62° to 64°N	12° to 8°W	119	38	0.32	3.13
Mean					0.49	2.20 (3)
April 16-21, 1968	52° to 42°N	5° to 10°W	89	71	0.79	1.27
Mean					0.79	1.27 (1)
Sept. 10-14, 1968	39° to 42°N	25° to 14°W	27.3	23.5	0.86	1.16
Sept. 15-19, 1968	42° to 40°N	14° to 12°W	29.5	33.2	1.13	0.88
Oct. 5-9, 1968	40°N	12° to 10°W	45.2	20.5	0.45	2.22
Oct. 21-26, 1968	39° to 42°N	10° to 13°W	28.1	20.8	0.74	1.35
Oct. 27-31, 1968	42° to 43°N	13° to 15°W	34.9	20.9	0.60	1.67
Nov. 1-5, 1968	43°N	15° to 14°W	33.6	20.9	0.62	1.61
Nov. 6-7, 1968	43° to 42°N	14° to 11°W	25.5	24.1	0.95	1.05
Mean					0.76	1.42 (7)
Overall Mean					0.76	1.49 (36)
Reciprocal						0.67

These results were kindly provided to us for use in this paper by Wolfgang Weiss of Freiburg, West Germany. The data are grouped below according to the areas in which they were measured (See Figure 2).

†TU is tritium unit.

Work is continuing at GISS to explore the tritium transport question.

For the sake of completeness, however, the analysis of Weiss and Roether [1980] should be examined in detail. First consider the assumption of isotopic equilibrium between vapor and precipitation over the ocean, perhaps the weakest link in their argument. The observational data they used to support the assumption are provided in Table 5. The data take the form of tritium concentrations

in paired vapor/precipitation samples collected in the North Atlantic during the period 1966 to 1968. The vapor samples were collected continuously over fixed time intervals and were paired with samples of rain which fell during these intervals. At complete isotopic equilibrium, and with their assumed value of 1.12 for α, the value of (T/H vapor)/(T/H rain) would be 0.89; Weiss and Roether considered the observed ratios in Table 5 to roughly approximate this value. For the listed measurements, however, the average ratio of tritium concentration in vapor to that in rain is 0.76. (Only 36 of the 37 listed measurements were used to produce this result; the T/H ratio in rain recorded on August 30 to September 3, 1966, appears anomalous and was thus not considered. The average (T/H vapor)/(T/H rain) ratio when this value is included is 0.81.) If 0.76 rather than their equilibrium value of 0.89 is adopted, the implied tritium input ratio is reduced from 2.4 to 2.0.

Since the tritium concentrations in vapor tend to be more nearly uniform than those in precipitation in Table 5, it can be argued that the average ratio of tritium concentration in precipitation to that in oceanic vapor should be found instead. The reciprocal of this average ratio could then be compared to the isotopic equilibrium value of 0.89. When processed in this fashion, the 36 measurements in Table 5 suggest a (T/H vapor)/(T/H rain) ratio of 0.67. The tritium input ratio implied by the observations would then be reduced from 2.4 to 1.8.

In truth, the proper way to process the observational data is not obvious. The data in the table are highly variable. It seems clear, though, that the observations suggest an average (T/H vapor)/(T/H rain) ratio less than the assumed 0.89.

Furthermore, the data presented in Table 5 are not necessarily representative of the northern hemisphere oceans. As shown in Figure 2, the samples were all collected in the east Atlantic. As seen in Table 5, many of the higher (T/H vapor)/(T/H rain) values were collected not far from the coast of Europe; perhaps continental effects played an important role.

Other important aspects of Weiss and Roether's analysis to consider are the latitude-dependent precipitation (P), evaporation (E), and tritium concentration in precipitation (C_p) values and the assumed uniform values of h and isotopic fractionation factor α. Although these quantities are known to vary strongly with season, Weiss and Roether employ annual averages and therefore might miss important seasonal correlations. For example, as shown in Figure 3, summer is by far the most important season for tritium input. In northern hemisphere mid-latitudes, estimates of summer evaporation rates over the oceans [Peixoto and Oort, 1983], which, by the way, roughly match the July evaporation rates produced in simulation 1, are about half the observed mean annual evaporation rates. The use of the larger annual rates in equation (1) could therefore lead to an overestimate of the vapor exchange input of tritium into the ocean.

The overestimation, however, might be counteracted by the use of 0.74 as the annual mean value of h in equation (1), which is significantly lower than observed summer values over the ocean [van Loon, 1984]. It is difficult to predict the net

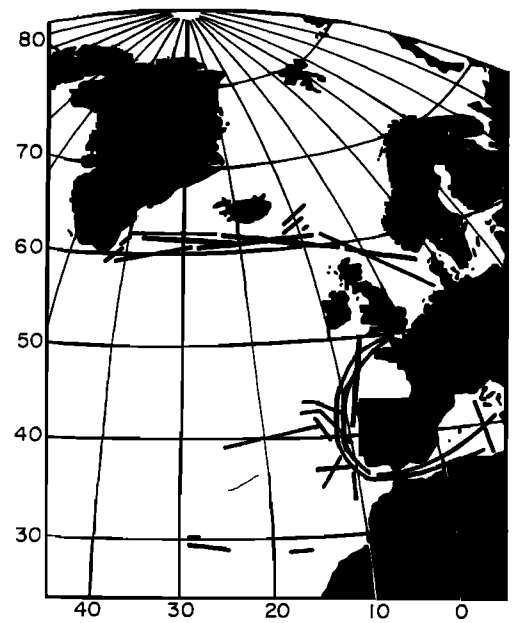

Fig. 2. Map showing the locations of the traverses along which Weiss and Roether obtained vapor/precipitation pairs for tritium analysis (see Table 5).

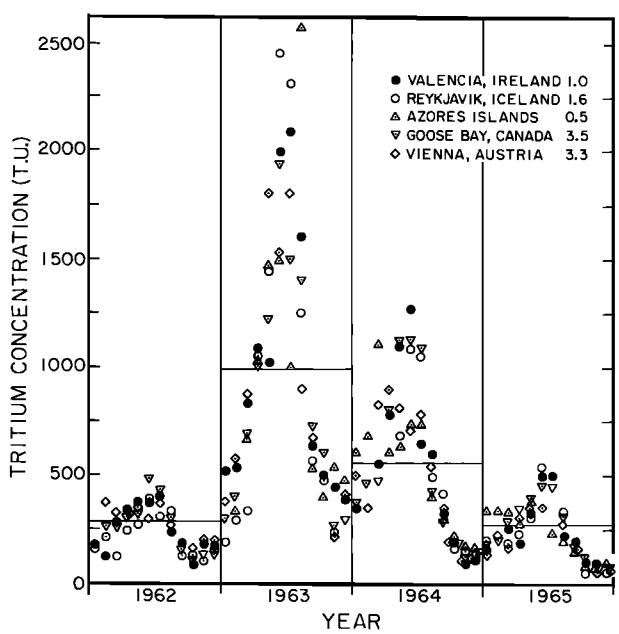

Fig. 3. Seasonal trend in the T/H ratio in rain at five localities before, during, and after the peak fallout year (1963). The measurements at Reykjavik, Azores, Goose Bay, and Vienna have been normalized to yield the same mean as Valencia. The normalization factors are listed in the figure (i.e., the Reykjavik results were all divided by 1.6, etc.). The annual means selected by Weiss and Roether [1980] for Valencia are shown for comparison. Concentrations are in tritium units (TU).

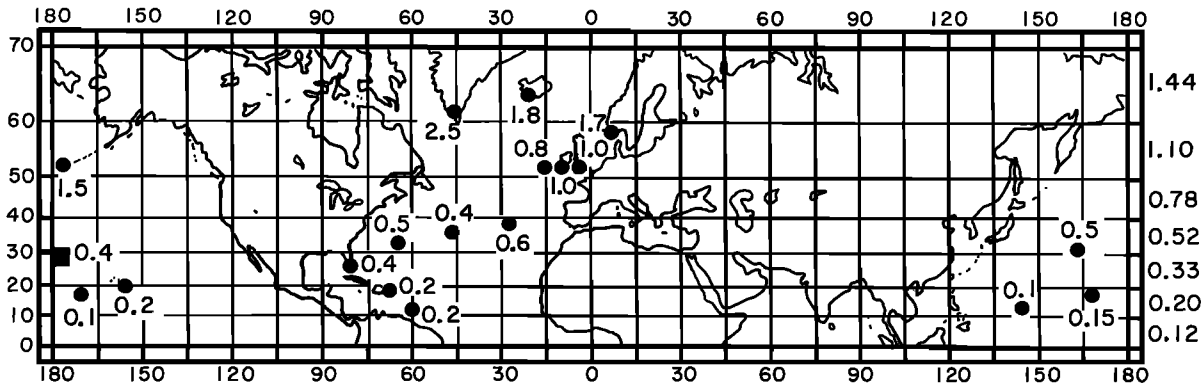

Fig. 4. Map showing the locations (circles) of the 18 sites used by Weiss and Roether to assess the T/H ratio distribution for oceanic rain. Shown by each point is the ratio of the local T/H ratio to that for Valencia, Ireland, rain. Also shown is the value for the Midway station (square) not used by Weiss and Roether. Shown on the right are the averages estimated by Weiss and Roether for 10° latitude belts based on the results for these ocean stations. These values are also referenced to Valencia, Ireland.

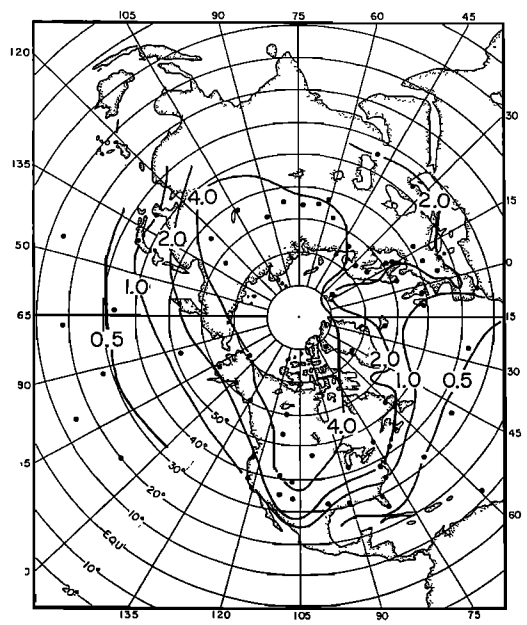

Fig. 5. Map showing the geographic distribution of T/H ratios for precipitation in the northern hemisphere. The average T/H ratios are referenced to that for Valencia, Ireland. The solid circles designate the locations of the sampling stations. The normalized T/H ratios for these stations are summarized in Table 7.

effect of using annual evaporation rates and h values on the computed vapor exchange input of tritium. Other seasonalities may also be important; oceanic precipitation rates in summer (Peixoto and Oort [1983], citing Jaeger [1976]) are reduced from their annual mean values, though not by as much as the evaporation rates, and values for alpha should decrease in summer. In a previous publication focusing on the North Atlantic [Weiss et al., 1979], Weiss and Roether mention that seasonal effects effectively cancel out, allowing for the use of annual means. They do not mention the extent to which this cancellation is fortuitous and whether or not it also applies to the Pacific Ocean. In a more complete analysis, monthly tritium inputs would be calculated.

The sparseness of evaporation and precipitation measurements over the oceans must also be considered, as should the small number of ocean stations used to estimate values of C_p (see Figure 4). Furthermore, as shown in Figure 5, strong continent-to-ocean gradients are inherent in the global field of T/H ratio in precipitation; this complicates the task of determining the effective average ratio over the ocean for a latitudinal band.

4.3. Oceanic Tritium Inventory Measurements

Tritium inventories measured as part of the GEOSECS survey (see Broecker et al. [1986] for summary) lend support to the Weiss and Roether scenario of tritium delivery. As summarized in Table 6, by subtracting the Weiss and Roether estimates of tritium delivery by precipitation and river runoff from the observed ocean tritium inventories, independent estimates of tritium input via vapor impact can be obtained. (This assumes a negligible upward flux of tritium vapor at the ocean surface.) These values can in turn be divided by the Weiss and Roether precipitation input values to produce independent estimates of the tritium input ratio. As shown in Table 6, a tritium input ratio of 3.8 is obtained with this method for the North Atlantic, and a tritium input ratio of 2.2 is obtained for the North Pacific. These ratios can be compared to the values 2.9 for the Atlantic and 2.0 for the Pacific obtained by Weiss and Roether [1980] using the Craig and Gordon [1965] equation. The two observational ratio estimates for the Pacific agree quite well, while the inventory-based ratio for the Atlantic is quite high. The inventory-based ratio for the two oceans combined is higher than that predicted by the GCM.

Again, the discrepancy may certainly result from the GCM's inability to transport tritium realistically. Possible problems with the inventory analysis, however, should also be noted. The precipitation input of tritium into the ocean is especially difficult to estimate; not only are

TABLE 6. Comparison of Tritium Inputs by Runoff and Precipitation

	North Atlantic, 10^{27} atoms	North Pacific, 10^{27} atoms	Total Northern Ocean, 10^{27} atoms
Observed ocean inventory	10.9	11.5	22.4
Precipitation input	2.0	3.2	5.2
Runoff input	1.3	1.1	2.4
P + R	3.3	4.3	7.7
Apparent vapor input i.e., (I - P - R)	7.6	7.1	14.7
Apparent vapor input / Precipitation input	3.8	2.2	2.8

As estimated by Weiss and Roether [1980] with the ocean inventory of tritium measured as part of the GEOSECS (see Broecker et al. [1986] for summary). The entries are decay-corrected to the year 1981.

precipitation measurements over the oceans sparse, leading to varying estimates of ocean precipitation in the literature [e.g., Baumgartner, 1982], but few measurements of tritium concentration in precipitation were taken in the center of the North Pacific and North Atlantic oceans (see Figure 4), where most ocean precipitation falls. Ascertaining the precipitation input of tritium along continental margins is also difficult, due to the strong continent-to-ocean gradient in tritium concentration. (See Figure 5.) Notice that with the inventory method, any underestimation of the precipitation tritium input necessarily leads to a corresponding overestimation of the vapor exchange input, resulting in a greater overestimation of the tritium input ratio.

Large, localized precipitation fluxes of tritium may also have occurred in the past, and if these fluxes were not measured, the total precipitation input of tritium would be further underestimated. Precipitation near the explosion sites immediately after the nuclear tests, for example, perhaps contained much higher tritium concentrations than those indicated in Figure 4, due to the scavenging of explosion-generated particulates and aerosols. One might even speculate that the Soviet tests in Siberia added significant quantities of tritium to the Arctic Ocean and that this tritium later found its way into the Atlantic. It would indeed be unfortunate for those who wish to use bomb-produced tritium as a global tracer if such local inputs are important to the global inventory; perhaps studies such as this will encourage the release of pertinent information by the nations that conducted major tritium-generating tests.

4.4. Continental Versus Oceanic T/H Ratios in Precipitation

Table 7 lists the relative tritium concentrations in precipitation observed at various northern hemisphere sites, and Figure 5 provides a geographical contour map constructed from these values. Continental precipitation in the real world is clearly characterized by higher T/H ratios than those found in oceanic precipitation. The question then arises as to whether this large contrast can be reproduced in the GCM.

The fourth and fifth columns of Table 3 for simulation 1 show that for the standard simulation, with the tritium source in the upper troposphere, there is no such distinction between oceanic and continental rains. This is due, at least in part, to the prevention in the model of tritium reevaporation from the ground surface. In the real world, tritium-laden precipitation water reaching a land or ice surface can reevaporate and thereby increase the T/H ratio in lower atmospheric layers. This would in turn increase the T/H ratio in subsequent precipitation events. Thus, one might conclude that the control simulation is not designed to compare tritium concentrations in continental and oceanic precipitation.

The results of simulation 6, however, can be considered; this simulation used a continental tritium source and thus could account directly for the effects of reevaporated tritium. The average ratio of tritium concentration in continental precipitation to that in oceanic precipitation for simulation 6 is about 4. (See the fourth and fifth columns of Table 3.) The corresponding ratio derived from observations, when potentially biased high-altitude stations are ignored, somewhat agrees with this value; it lies between 3 and 4 at all latitudes. Simulation 6, however, represents the extreme case in which all the tritium is added from the continents. It thus maximizes the ocean-continent difference in T/H ratios. If a realistic simulation were run in which tritium inputs from both the stratosphere and the continents were included in their proper proportions, the contrast between the T/H ratio in continental and oceanic rains could be considerably smaller than that indicated by observations.

5. Summary and Conclusions

GCM simulations of tritium transport from the upper atmosphere to the ocean have been performed in an attempt to assess the ratio of tritium input into the ocean via vapor impact to that via precipitation. The results are quite insensitive to

TABLE 7. Locations of Stations at Which a Sufficiently Complete Record of Tritium Content in Precipitation Exists to Permit Comparison With the Reference Station at Valencia, Ireland

Station	Latitude	Longitude	$\frac{T/H}{T/H_{Valencia}}$
Nord, Greenland	82°N	17°W	5.9
Isfjord, Norway	78°N	14°E	2.0
Thule, Greenland	77°N	69°W	6.3
Barrow, Alaska	71°N	157°W	3.7
Pelkosenniemi, Finland	67.1°N	27.5°W	3.8
Arjeplog, Sweden	66.0°N	17.9°E	3.0
Archangelsk, U.S.S.R.	65°N	41°E	3.5
Reykjavik, Iceland	64.1°N	21.9°W	1.8
Jakutsk, U.S.S.R.	62°N	130°E	6.3
Palmer, Alaska	61.6°N	149.1°W	3.5
Groennedal, Greenland	61.2°N	48.1°W	2.5
Bethel, Alaska	60.8°N	161.8°W	2.1
Whitehorse, Canada	60.7°N	135.1°W	4.7
Fort Smith, Canada	60.0°N	112.0°W	4.0
Huddinge, Sweden	59.2°N	18.0°E	2.0
Lista, Norway	58.1°N	6.6°E	1.7
Perm, U.S.S.R.	58°N	56°E	4.9
Enisejsk, U.S.S.R.	58°N	92°E	6.7
Goteburg, Sweden	57.7°N	18.0°E	2.0
Salehard, U.S.S.R.	55°N	66°E	4.9
Omsk, U.S.S.R.	55°N	73°E	5.3
Novosibirsk, U.S.S.R.	55°N	83°E	5.6
Skovordino, U.S.S.R.	54°N	124°E	6.0
Edmonton, Canada	53.6°N	113.5°W	5.6
Goose Bay, Canada	53.5°N	60.4°W	3.0
Petropavlosk,U.S.S.R.	53°N	159°E	2.1
Irkutsk, U.S.S.R.	52°N	104°E	7.4
Adak, Alaska	51.9°N	176.7°W	1.5
Milford Haven, United Kingdom	51.7°N	5.0°W	1.0
Valencia, Ireland*	51.9°N	10.3°W	1.0
Sindorf, West Germany	50.9°N	6.7°E	1.8
Stuttgart, West Germany	48.8°N	9.2°E	2.5
Vienna, Austria	48.3°N	16.4°E	2.7
Bismarck, North Dakota	46.8°N	100.8°W	4.6
Portland, Oregon	45.6°N	122.6°W	1.6
Ottawa, Canada	45.3°N	75.7°W	3.0
Grenoble, France	45.2°N	5.3°E	3.0
Genoa, Italy	44.2°N	8.6°E	1.3
Boston, Massachusetts	42.4°N	71.0°W	2.0
Chicago, Illinois	41.8°N	87.8°W	2.7
Salt Lake City, Utah	40.8°N	112.0°W	4.3
Denver, Colorado	39.8°N	104.9°W	5.0
Washington, D. C.	38.8°N	77.0°W	2.0
Punta del Gado, Azores	37.8°N	25.7°W	0.6
Menlo Park, California	37.4°N	122.1°W	1.0
Adana, Turkey	37.0°N	35.3°E	2.5
Pohang, South Korea	36.0°N	129.4°E	1.0
Tokyo, Japan	35.7°N	139.8°E	1.0
Teheran, Iran	35.6°N	51.3°E	2.0
Cape Hatteras, North Carolina	35.3°N	75.6°W	1.0
Flagstaff, Arizona	35.1°N	111.7°W	2.8
Weathership E	35.0°N	48.0°W	0.4
Albuquerque	35.0°N	106.6°W	3.0
Santa Maria, California	34.9°N	120.4°W	0.8
Weathership V	34.0°N	164.0°E	0.5
Bermuda	32.4°N	64.7°W	0.5
Waco, Texas	31.6°N	97.2°W	1.0
Gibraltar, United Kingdom	31.3°N	5.4°W	≈1.1
Baton Rouge, Louisiana	30.5°N	91.1°W	≈0.7
Ocala, Florida	29.2°N	82.1°W	0.3
Midway Island	28.2°N	177.4°W	0.4
Miami, Florida	25.8°N	80.2°W	0.4
Wake Island	19.3°N	166.6°E	0.2

TABLE 7. (continued)

Station	Latitude	Longitude	$\frac{T/H}{T/H_{Valencia}}$
Hilo, Hawaii	19.7°N	155.1°W	0.2
San Juan, Puerto Rico	18.4°N	66°W	0.2
Johnston Island	16.7°N	169.5°W	0.1
Guam	13.5°N	144.8°E	0.1
Barbados	13.1°N	59.5°W	0.2

Values are from International Atomic Energy Agency [1970, 1971] and Ostlund [1982].
*Reference station.

the tritium source location and to changes in the parameterizations of model physics. These simulations indicate that when the continental precipitation/reevaporation pathway is included, the ratio of tritium delivery by vapor to that by precipitation is about 1.1.

This ratio is less than half that obtained from observational data either by the use of the Craig-Gordon equation (assuming isotopic equilibrium between vapor and precipitation) or by subtracting the precipitation and runoff contributions from the observed ocean inventories. Hence there is a major conflict between the general circulation model simulation of tritium delivery to the ocean and the observation-based perception of how it actually happened. The discrepancy between the model result and real world appearance is reduced when existing direct comparisons of T/H ratio in vapor and rain are taken at face value. Still, a major difference remains between the model-based and observation-based estimates.

As a result of the simulations described above as well as many additional sensitivity simulations, the authors feel confident that no simple adjustment of the GISS model parameterizations will produce an input ratio consistent with the observational value. One of two situations must apply. First, the model may fail to account properly for some important tritium transport process in the atmosphere. Second, the observational data may not be complete. Measurements of tritium in precipitation, for example, may be inadequate, and local fallout of tritium immediately after the bomb tests may have gone unnoticed. Neglected seasonal correlations in the observational analysis may also be important. Further study of the tritium transport problem is certainly warranted. The GCM simulations may serve as a useful alternative means of examining tritium transport.

Acknowledgments. The reviewers' comments are appreciated. Ms. Vicky Costello typed and edited the manuscript. Climate modeling at GISS is supported by the NASA Climate Program.

References

Arakawa, A., Design of the UCLA general circulation model, Tech. Rep. 7, 116 pp., Dep. of Meteorol., Univ. of Calif., Los Angeles, 1972.

Baumgartner, A., Water balance, in Land Surface Processes in Atmospheric General Circulation Models, edited by P. S. Eagleson, 515-538, Cambridge University Press, New York, 1982.

Baumgartner, A., and E. Reichel, Die Weltwasserbilanz, 179 pp., Oldenbourg Verlag, Munich, 1975.

Broecker, W. S., T.-H. Peng, and G. Ostlund, The distribution of bomb tritium in the ocean, J. Geophys. Res., 91, 14,331-14,344, 1986.

Craig, H., and L. I. Gordon, Deuterium and oxygen 18 variations in the ocean and the marine atmosphere, in Stable Isotopes in Oceanographic Studies and Paleotemperatures, Spoleto Conference Proceedings, edited by E. Tongiorgi, pp. 9-130, Consiglio Nazionale delle Richerche Laboratorio di Geologia Nucleare, Pisa, 1965.

Ehhalt, D. H., Vertical profiles and transport of HTO in the troposphere, J. Geophys. Res., 76(30), 7351-7367, 1971.

Federer, B., N. Brichet, and J. Jouzel, Stable isotopes in hailstones, I, The isotopic cloud model, J. Atmos. Sci., 39(b), 1323-1335, 1982.

Hansen, J., G. Russell, D. Rind, P. Stone, A. Lacis, S. Lebedeff, R. Ruedy, and L. Travis, Efficient three-dimensional global models for climate studies: Models I and II, Mon. Weather Rev., 111, 609-662, 1983.

International Atomic Energy Agency, Environmental Isotope Data, 2, World Survey of Isotope Concentration in Precipitation (1964-1965), Tech. Rep. Ser. 117, Vienna, 1970.

International Atomic Energy Agency, Environmental Isotope Data, 3, World Survey of Isotope Concentration in Precipitation (1966-1967), Tech. Rep. Ser. 129, Vienna, 1971.

Jaeger, L., Monatskarten des Niederschlags fuer die ganze Erde, Ber. Dtsch. Wetterdienstes, 18 (139), 38 pp., 1976.

Jouzel, J., L. Merlivat, and E. Roth, Isotopic study of hail, J. Geophys. Res., 80, 5015-5030, 1975.

Jouzel, J., G. Russell, R. Suozzo, R. Koster, J. W. C. White, and W. S. Broecker, Simulations of the HDO and $H_2{}^{18}O$ atmospheric cycles using the NASA/GISS general circulation model: The seasonal cycle for present day conditions, J. Geophys. Res., 92, 14,739-14,760, 1987.

Koster, R., J. Jouzel, R. Suozzo, G. Russell, W. Broecker, D. Rind, and P. Eagleson, Global sources of local precipitation as determined by the NASA/GISS GCM, Geophys. Res. Lett., 13, 121-124, 1986.

Koster, R., P. Eagleson, and W. S. Broecker, Tracer water transport and subgrid precipitation variation within atmospheric general circulation models, Tech. Rep. 317, 364 pp., Ralph M. Parsons Lab., Dep. of Civ. Eng., Mass. Inst. of Technol., Cambridge, 1988.

Merlivat, L., Molecular diffusivities of $H_2{}^{16}O$, $HD^{16}O$, and $H_2{}^{18}O$ in gases, J. Chem. Phys., 69, 2864-2871, 1978.

Ostlund, H. G., The residence time of the freshwater component in the Arctic Ocean, J. Geophys. Res., 87, 2035-2043, 1982.

Peixoto, J. P., and A. H. Oort, The atmospheric branch of the hydrological cycle and climate, in Variations in the Global Water Budget, edited by A. Street-Perrott, M. Beran, and R. Ratcliffe, pp. 5-65, D. Reidel, Hingham, Mass., 1983.

Rind, D., Dependence of warm and cold climate depiction on climate model resolution, J. Clim., 1, 965-997, 1988.

Russell, G., and J. Lerner, A new finite-differencing scheme for the tracer transport equation, J. Appl. Meteorol., 20, 1483-1498, 1981.

Taylor, C. B., The vertical variations of isotopic concentrations of tropospheric water vapor over continental Europe, and their relationship to tropospheric structure, Rep. INS-R-107, Inst. of Nucl. Sci., Lower Hutt, New Zealand, 1972.

van Loon, H. (Ed.), World Survey of Climatology, vol. 15, Elsevier, New York, 1984.

Weiss, W., and W. Roether, The rates of tritium input to the world oceans, Earth Planet. Sci. Lett., 49, 435-446, 1980.

Weiss, W., W. Roether, and E. Dreisigacker, Tritium in the North Atlantic Ocean: Inventory, input and transfer into deep water, in The Behavior of Tritium in the Environment, pp. 315-336, International Atomic Energy Agency, Vienna, 1979.

W. S. Broecker, Lamont-Doherty Geological Observatory of Columbia University, Palisades, NY 10964.

J. Jouzel, Laboratoire de Geochimie Isotopique, CEA/IRDI/DESICP, Saclay, 91191 Gif-sur-Yvette, CEDEX, France.

R. D. Koster, Code 624, NASA Goddard Space Flight Center, Greenbelt, MD 20771.

D. Rind, G. L. Russell, and R. J. Suozzo, Goddard Institute for Space Studies, 2880 Broadway, New York NY 10025.

J. W. C. White, University of Colorado, INSTARR Box 450, Boulder, CO 80303.

(Received July 27, 1988;
revised March 10, 1989;
accepted March 22, 1989.)